

CHAPTER-III

MAGNETIC PROPERTIES

MAGNETIC PROPERTIES

INTRODUCTION:

Magnetisation is one of the most fundamental property of ferrites . The saturation magnetisation, coercivity and remanance are studied with the help of hysteresis. Besides these, ferrites exhibit properties of swithing and memory. The magnetisation is the net result of antiparallel magnetic moment of the cation per unit volume of material which is induced in it when placed in external magnetic field. When magnetisation occurs even in the absence of external field, called spontaneous magnetisation and it is the most striking property of magnetic material. The saturation magnetisation within the domain is maximum that can be achieved in the material at given temperature. The origin of magnetisation lies in aligning forces due to an internal magnetic field called weiss field [1]. However, quantum mechanics relates this to the Hesenberg's exchange forces [2]. The value of saturation magnetisation (M_s) plays an important role in application of ferrites like, low value of M_s required in microwave application while high value of ' M_s ' depends on the cations present and their distribution.

In ferrites, the study of hysteresis gives valuable data on saturation Magnetisation (M_s), coercive forces (H_c), and remanance ratio(M_r/M_s) Therefore, the magnetic parameters related to hysteresis, help to decide the nature of application of ferrites.

The wide range of values of permeability of ferrite makes suitable for various frequency range applications. Magnetic susceptibility is the most convinient and useful property. The ac susceptibility χ_{ac} often shows intricate properties. The shape of $\chi_{ac} \times T$ curves demonstrate the existance of domain states and spin glass state [3] which needs to be confirmed again by Mossbauer or Neutron diffraction studies.

Ferrites exhibit the properties of ferromagnetics in which the spontaneous magnetisation is maximum at absolute zero. If the temperature increases, the spontaneous magnetisation decreases and at particular temperature the transition from ferromagnetic phase to paramagnetic phase occurs. This temperature is called Curie temperature. According to Neel and Gorter the Curie temperature of ferrites depends on distance of metallic ions on two sites A and B.

In this chapter, the studies of magnetisation, hysteresis, susceptibility, Curie temperature are discussed.

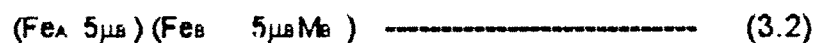
3.1 MAGNETISATION IN FERRITES:

The magnetisation of a solid material as a whole, is a vector sum of magnetisation of each of domains, the contribution of each being weighed by its fraction of total volume. Thus the net magnetisation of the solid ranges from zero, if the weighed vector sum is zero, the net magnetisation is maximum, if the solid is single domain with all the atomic moments aligned in a given direction.

The magnetisation in spinel structure can be explained on the basis of Neel's two sublattice model to a large extent. The normal spinel ferrite is non magnetic. For the inverse spinel ferrite the magnetisation can be deduce as,



The net moment is only due to M^{2+} divalent metal ions as the Fe^{3+} ions on A sites are coupled with their spins antiparallel to those of Fe^{3+} ions on B sites.



Suppose M, a transition element with n electrons in the d-shell, the magnetic moment per unit formula is $(n\uparrow\mu_B)$ or $(10-n)\mu_B$ depending on d-shell which is filled less than half or more than half respectively. The degree of inversion is fraction of X of the divalent metal ions that are on B-site. The arrangement of moment could be written as

$$[(1-X)M \chi Fe] [(1-\chi)Fe_B x M] \text{ --- (3.3)}$$

and the net magnetic moment is given by the difference between moments on A site and B site as,

$$\mu_B = M(1-2X) - 10(1-X) \text{ --- (3.4)}$$

For normal spinel $X=0$.

and for inverse spinel $X=1$.

3.2 MAGNETIC INTERACTIONS IN FERRITES :

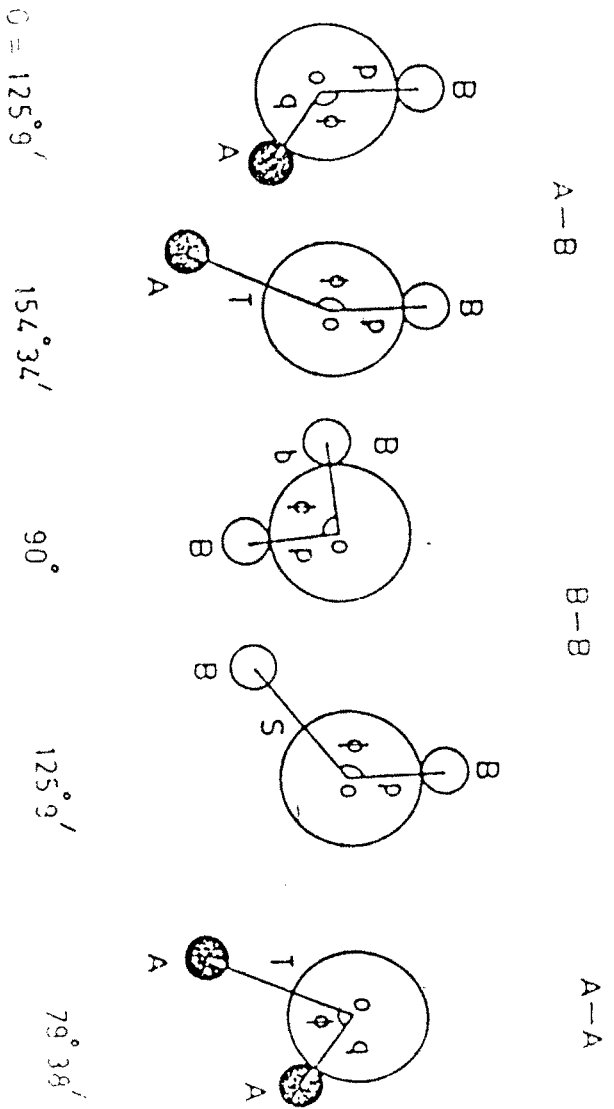
Three kinds of magnetic interactions are possible in ferrites, between the metallic ions through intermediate O^{2-} ions by superexchange mechanism namely, A-A, B-B and A-B interactions. The magnitude of interaction energy depends on angle between $Me^I - O - Me^{II}$ and the distance from these ions to oxygen ion. An angle of 180° will give rise the highest exchange energy and the energy decreases rapidly with increasing distances. The various possible configurations of the ion pairs in spinel ferrites with favourable distances and angles for an effective magnetic interaction as envisaged by Gorter (4) and as shown in fig 3.1. Out of these configurations A-B interaction is predominant, B-B interaction is intermediate and A-A interaction is the weakest, as both distances and angle between two ions are not favourable.

3.3 HYSTERESIS :

According to Weiss the random orientation of tiny magnetic domains would lead to zero magnetisation. The net magnetisation exhibited in the presence of small applied magnetic field is a consequence of orientation of direction of magnetic domains in the direction of applied magnetic field.

The magnetisation will increase in applied magnetic field and reaches to a saturation value at certain critical field. The curve OABC Fig 3.2 is called magnetising curve. If the magnetising field is reduced to zero and an increasing reverse field is applied,

FIG. 3-1 ANGLE BETWEEN A-A, B-B & A-B CATIONS IN A SPIRAL STRUCTURE



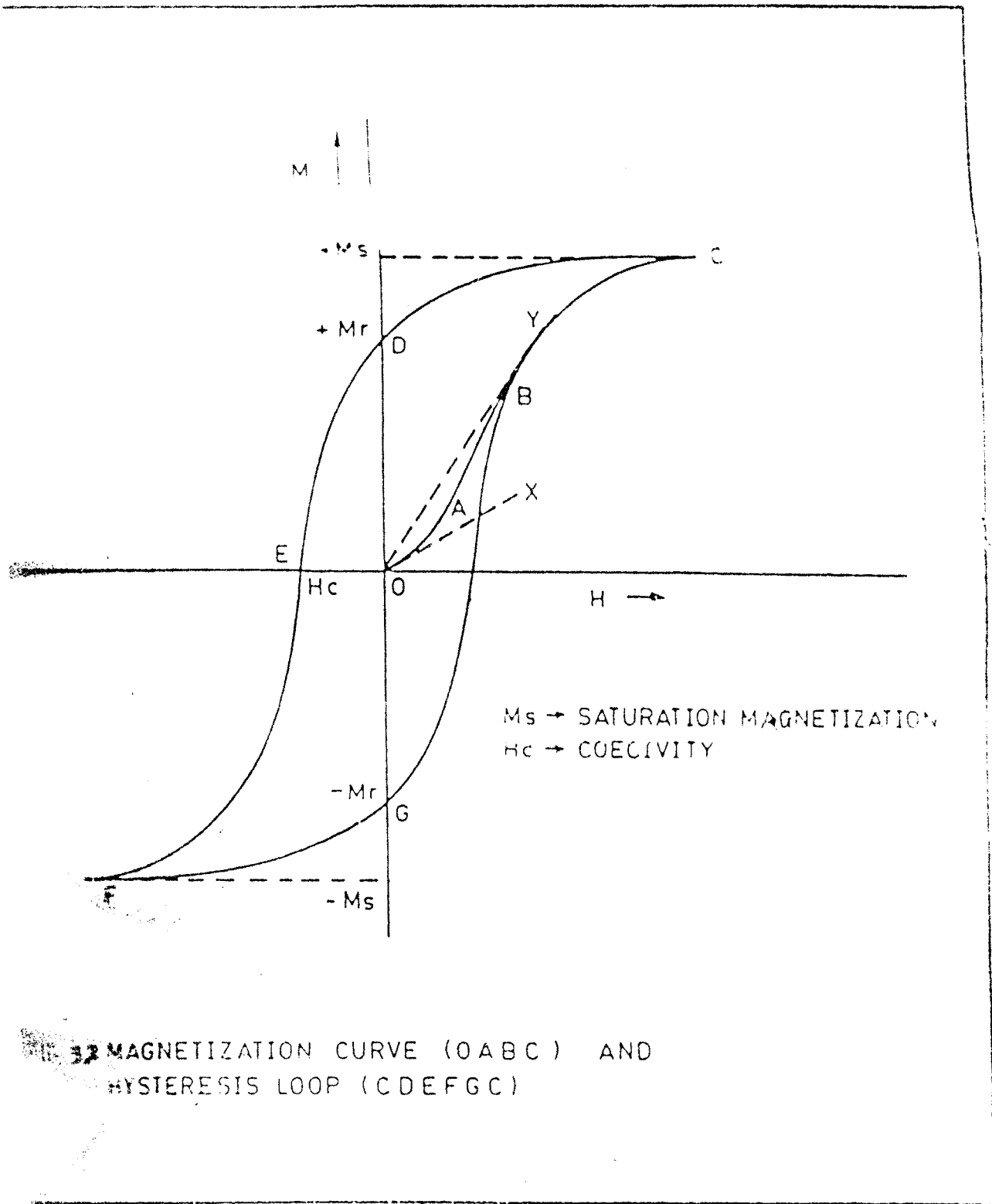


FIG. 32 MAGNETIZATION CURVE (OABC) AND Hysteresis LOOP (CDEFGC)

the original magnetization curve OABC is not followed, but a lag of magnetisation to the magnetizing field occurs. Increase in the reverse field leads to saturation in reverse direction and if the field is again returned to the original direction, the complete cyclic loop CDEFGC (Hysteresis) is obtained as shown in Fig 3.2 .

In order to discuss the suitability of electrical and electronic applications to describe the magnetization process in a quantitative manner [5]. The cyclic loop relates directly to a.c. applications. The area inside the loop is indicative of losses occurring due to traversal of the loop.

The magnitude of initial susceptibility χ_0 and the maximum susceptibility is determined by the slope of the tangent to the magnetizing curve. Initial permeability can be measured by hysteresis loop, if the magnetic induction is plotted against magnetising field. The coercive field H_c is required magnetising field to demagnetise the specimen completely from retentivity (M_r). Then retentivity is the residual magnetization at zero field. The saturation magnetisation is given by the point 'C' of the loop. The coercive field is found to vary from 10^{-1} to 10^{+3} Oe[6].

The hysteresis loop of micropowder can be classified in four types [7] as

- | | |
|--------------------------|---------------------------|
| 1) Multy Domain (MD) | 2) Singel Domain (SD-UA) |
| 3) Singel Domain (SD-CA) | 4) Superparamagnetic (SP) |

Hysteresis properties, are mainly dependant on chemical composition, heat treatment, crystal structure, cation distribution, atmosphere of sintering and final fabrication. Experimental techniques for the measurement of magnetic properties are described by Maxwell [8]. Hysteresis loop can be traced out with the help of hysteresis loop tracer.

3.4 SUSCEPTIBILITY :

The susceptibility is defined as the ratio of the magnetization (M) produced in the substance to the applied magnetic field (H) as

$$K = M / H \quad \text{emu} / \text{cm}^3 \text{ Oe} \quad \text{-----} \quad (3.5)$$

Since M is the magnetic moment per cm^3 , K is called volume susceptibility.

The mass susceptibility (χ) is defined as

$$\chi = K / \rho \quad \text{emu} / \text{g Oe} \quad \text{-----} \quad (3.6)$$

$\rho = \text{Density}$

Of all intrinsic properties characterising a magnetic substance, magnetic susceptibility is the most convenient and useful one, for extracting many important information related to physical, chemical and magnetic state of substance.

Susceptibility study is very useful in order to invoke the grain size effects like a very fine stable SD particles become SP particles on heating to temperature of several degree below the curie temperature. When the thermal energy of SD particles become comparable to the effective magnetic anisotropy energy, SD particle called superparamagnetic (SP). Under these conditions, magnetisation direction fluctuate between the easy axes of the grain. In such a state, the grain is said to exhibiting superparamagnetisation, and for the volume (V) of the grain the temperature is referred to as blocking temperature (T_b), which will be less than curie temperature (T_c) of the material. The volume (V), the saturation magnetisation (J_s) and coercive force (H_c) are related by Neel [9] as

$$V J_s H_c = 2KT_b \quad \text{-----} \quad (3.7)$$

Where K -- Boltzman constant.

Thus, the SP can be change to SD by cooling below their T_b .

The susceptibility become infinite and the spontaneous magnetisation appears at particular temperature called curie or Neel temperature. The transition from ferro to paramagnetic region is not sharp in each case but gives tailing effect due to spin clusters (i.e. short range spin ordering).

The low field a.c. susceptibility plays an important key role in the study of spin glass behaviour. The cusp at low temperature [10,11], sudden change in $\chi_{ac} - T$ curve as well as value of χ_{ac} [12] or maxima [13] in the low field a.c. susceptibility versus temperature Characterise the spin glass behaviour.

3.5 CURIE TEMPERATURE :

In ferromagnetics the domain ordering is due to presence of internal molecular field as is found to be maximum at 0°K. Therefore, the spontaneous magnetisation is found to be maximum at absolute zero.

The spontaneous magnetisation decreases with increase in temperature. At curie temperature, the spontaneous magnetisation lost by the substance and the paramagnetic phase results. Thus curie temperature separates the disordered paramagnetic phase from the ordered ferromagnetic phase.

Forrster studied the $Ni_x Zn_{1-x} Fe_2O_4$ system to show the variation of curie temperature and AB interaction. Curie temperature of ferrites have been found to be closely related to $Fe^{3+} - O - Fe^{3+}$ and other magnetic linkage via the interaction energy per linkage [14]. Substitution of non-magnetic ion reduces the curie temperature. The relation between curie temperature and cation distribution is given by Gilileo [15].

3.6 MAGNETOSTRICTION :

Ferrites change their length when they are magnetized. This dimensional change of the crystal as a function of magnetization is known as magnetostriction and it plays an important role in domain geometry and in practical use of transformer materials.

The incremental change may be positive or negative for different materials at saturation. Most of ferrites exhibit negative incremental change except for few cases like Fe_2O_4 .

3.7 EXPERIMENTAL :

3.7.1 MAGNETISATION MEASUREMENTS :

The saturation magnetisation of samples were carried out by using the high fields hysteresis loop tracer. The instrument used for this measurement is shown in fig . 3. 3.

It consists of electromagnet and pick up coil . The pick up coil contains double coil with equal turns as well as area . when a. c. current is supplied to the electromagnet an alternating emf is produced in the coil . The induced emf is proportional to the magnetisation of the sample. The current was calibrated in terms of magnetic flux . Further details of given elsewhere [16] .

3 . 7 . 1 . 1 Calibration and Measurement of Saturation Magnetification :

The vertical displacement on c.r.o. is calibration for pure nickel sample of mass 0.2679 grams. The selective range calibration on oscilloscope is kept fixed on 0.1 volt per division for all samples . The current in control unit of power supply is 120 mA it gives vertical output of 0.27 v. As the standard magnetisation for the nickel sample is 53.34 emu/gm total magnification of nickel is .

$$53.34 \times 0.2679 = 14.2897 \text{ emu / v.}$$

Therefore calibration of height of the hysteresis loop on vertical displacement is given by calibration factor = 0 . 05292

The vertical displacement for each sample is noted by introducing each pellet separately into the air gap between the pole pieces. the saturation magnetification is calculated by the relation;

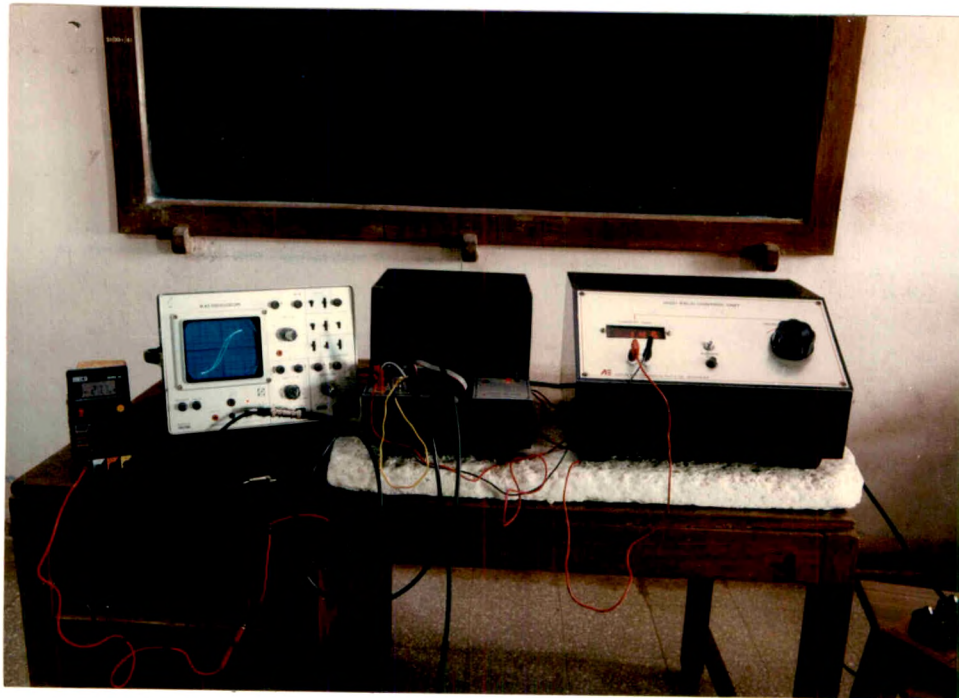


Fig.3.3 : Experimental Set-up of Hysteresis Loop Tracer

$$M_s = \frac{\text{vertical output in volts}}{\text{mass of sample}} \times \text{density emu / gm} \dots \dots \dots (3.8)$$

The magnetic moment per formula unit in B magnetons is given by.

$$\eta_B = \frac{M_s \times \text{mol. wt. of unit cell}}{5585 \times d_x}$$

where d_x = actual density of sample in gm / cc.

3.7.2 A.C. SUSCEPTIBILITY :

The low field a.c. susceptibility measurement of powdered samples were taken in temperature region 300--850°k using the double coil set up [17] shown in fig. 3.4, operating at a frequency of 263 hz and in v.m.s. field of 7 Oe.

The set up consist of two Helmholtz coil to produce uniform field at pick up coil. A furnace is fabricated by winding the platinum wire on silica tube is used to heat the sample. To avoid over heating of the coils a glass jacket with water circulation is used. The furnace is inserted in glass jacket which is placed in the center of pick up coil. Height of sample tube is maintained such a way that the sample can stay at the centre of the double coil. The current to the Helmholtz coil is supplied by an oscillator and a high quality power amplifier. The signal induced in the double coil, which is proportional to the rate of change of magnetic moment of the sample, is amplified, rectified and read out on digital voltmeter. The meter reading can be calibrated in term of magnetic moments. The temperature of furnace is maintained by power supply. The temperature was measured by calibrated platinum--platinum--rhodium thermocouple. The sample was gradually heated

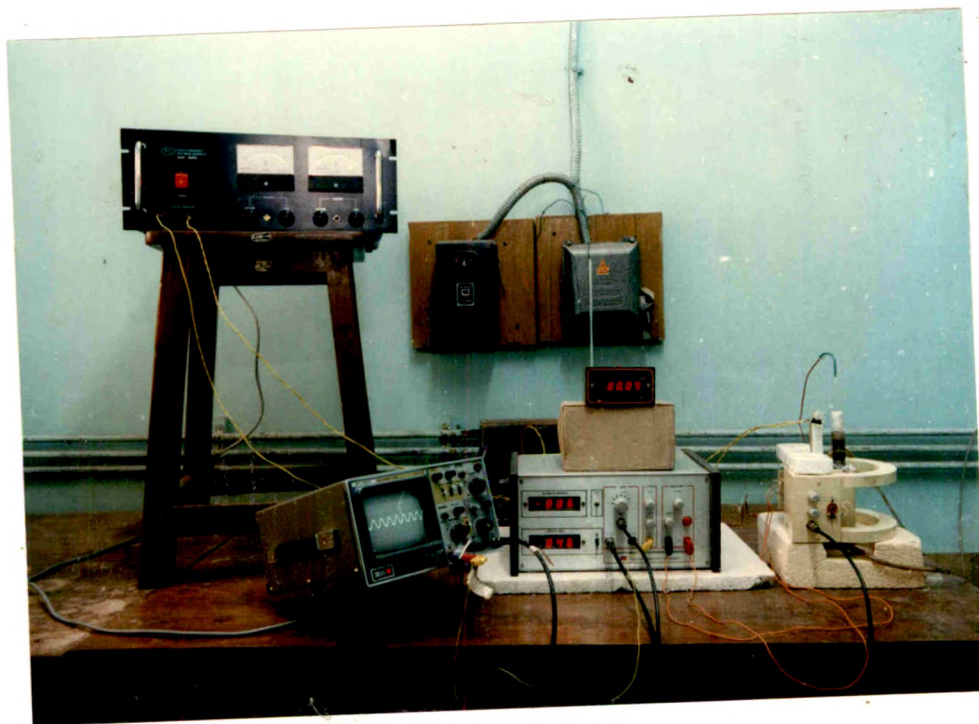


Fig.3.4 : Experimental Set-up of Low field A.C. Susceptibility Measurement

and at various temperatures the signal corresponding to the magnetic moment was recorded. The heating was continued till the signal was reduced to zero.

3.8 RESULTS AND DISCUSSION :—

3.8.1 MAGNETISATION AND MAGNETIC MOMENT :

The magnetisation study was made at room temp. with the help of hysteresis method. The saturation magnetisation ($4\pi M_s$) and magnetic moment n_B for these samples are given in table 3.1 . The curie temperatures of these samples are also noted in the same table. The values of $4\pi M_s$ and n_B for $MgFe_2O_4$ and $CuFe_2O_4$ nearly agree with the reported values.

In Zn containing Cu and Mg ferrites the magnetisation increases upto $Zn = 0.3$ and then decrease with increase of Zn content. In the series $Mg_xCu_{1-x}Fe_2O_4$ the magnetisation decreases with x. These observations are as expected and the magnetisation behaviour can be explained on the basis of Neel's molecular field model. According to this model A - B interaction is more effective and stronger than A - A and B - B interactions. The net magnetic moment of the lattice is given by the vector sum of the magnetic moments of A and B sublattice ($M = M_B - M_A$). In this model collinear arrangement of magnetic moments of individual sites is presumed i.e. the magnetic ions on each sublattice are ferromagnetically aligned.

The cation distribution for Zn containing ferrites can be written as $(Fe_{1-x}Zn_x) [Fe_{1+x}Mg_{1-x}]$ According to site preference energies given by Miller [14] , the Cu and Mg ions prefer B site and Zn ion occupy A site. The magnetic moment of this cation distribution is calculated by the formula (3.4) Basically there are three types of interactions in ferrites i.e A-A, A-B and B-B, where as A-B interaction is strongest one.

It was experimentally found that , the addition of small amount of Zn to $MgFe_2O_4$ causes the increase of magnetic moment. At Zn content higher than 0.3, the

Table No. 3.1 Compositional variation of magnetic moment and saturation magnetisation of mixed ferrites.

Sample	n_B (μ_B)	M_s emu/g	$4\pi M_s$
$MgFe_2O_4$	0.6334	59.44	746.56
$Mg_7Zn_3Fe_2O_4$	1.0182	101.01	1268.67
$Mg_4Zn_6Fe_2O_4$	0.6953	62.71	787.63
$Mg_7Zn_3Fe_2O_4$ (mixed)	0.7009	72.86	915.12
$Mg_4Zn_6Fe_2O_4$ (mixed)	0.3489	31.91	400.87
$Mg_7Cu_3Fe_2O_4$	0.4830	48.09	604.01
$Mg_4Cu_6Fe_2O_4$	0.7319	69.22	869.40
$Cu_7Zn_3Fe_2O_4$	1.8482	181.50	2279.64
$Cu_4Zn_6Fe_2O_4$	1.1793	97.15	1220.25
$CuFe_2O_4$	1.1910	122.28	1535.83

experimentally measured magnetic moment decreases more and more from the theoretical one [18,19] . The addition of Zn^{2+} ions forces the same number of Fe^{3+} ions from A-site to B-site, giving rise to higher ordering of ionic spins in B site as well as to the expected increase of the net magnetic moment. When the Zn content exceeds beyond 0.3 the saturation magnetisation decreases. This could be related to the decrease of Fe^{3+} ions on A-site giving rise to the reduction of A-B interaction . The ionic spins of B-site are no longer held parallel to one another and their angular orientation result in reducing the net magnetic moment . The η_B values are noted in table 3.1

Curie temperatures of these samples measured by a.c. susceptibility method are given in the same table curie temp decrease with increase of Zn content. The inclusion of non-magnetic ions Zn generally decreases the curie temp. curie temp. of ferrites have been found to be closely related to Fe_A-O-Fe_B linkages, its strength and angle between cations. In the present system addition of Zn reduces the strength of the linkages. Hence the decrease in curie temp.

From table 3.1 it is observed that the values of saturation magnetisation for the sintered samples are less than that of samples prepared by co-precipitation method. This may be due to different preparation conditions, their chemical inhomogeneity and density of the sample.

3.8.2 A.C. SUSCEPTIBILITY WITH TEMPERATURE :--

High temperature a.c. susceptibility measurement were first carried out on Iron by HOPKINSON [20] who showed that it reached a peak value just before T_c and become Zero rapidly. Applying this technique , Radhakrishnamurthy et al [21] have explored the complex magnetic behaviour of titanomagnetites. Ferrites have been studied by this method by many workers(21,22,23). Three types of peaks have been reported in χ_{ac} -T curves (i) Hopkinson peak is the one occurring just before the T_c of any magnetic materials in the multi domain states. (ii) Isotropic peak, which could be seen

clearly for a magnetic material in multidomain form and only if the material has a temp. at which the magneto crystalline anisotropy is zero. (iii) single domain peak which could be obtained only if the sample under investigation has a substantial proportion of single domain particles in it and occurs at the blocking temp. (T_b) of the particles.

Fig 3.(i) show the variation of χ_T with T for $Mg_{.7}Zn_{.3}Fe_2O_4$. curve (a) is for the sample prepared by co-precipitation method but not sintered (b) the same sample sintered at $600^\circ C$ and (c) at $900^\circ C$. The as it is sample show a continuous decrease of χ with temp. the susceptibility increases with temp. and show a maxima at $110^\circ C$ and then decreases and becomes zero at curie temp. for $600^\circ C$ sintered sample. The susceptibility remains constant near to curie temp. and decreases and becomes zero at curie temp. for the sample sintered at $900^\circ C$. From these observations and concepts discussed by other workers it can be interpreted that the as it is sample contains super paramagnetic particles. The tailing effect is more which may be due to inhomogeneous and amorphous nature of the sample. When a sample is sintered at $600^\circ C$ homogeneity can be achieved in larger extent and particle size also increases. This clearly indicates the single domain behaviour of the sample. At higher sintering temp. ($900^\circ C$) the particle size again increases and the sample behaves like multidomain type. The increase in particle size due to sintering is also confirmed by X-ray diffraction method. Similar observations are also made on mixed $Mg_{.7}Zn_{.3}Fe_2O_4$ ferrites. [fig. 3 (viii)]

Similar result is also observed in case of $Mg_{.7}Cu_{.3}Fe_2O_4$ shown in fig. [3(ii)]. This sample sintered at $600^\circ C$ contains M.D+SD behaviour where as MD behaviour for $900^\circ C$ sintered sample.

For the sample $Mg_{.4}Zn_{.6}Fe_2O_4$ and $Cu_{.4}Zn_{.6}Fe_2O_4$ the susceptibility continuously decreases with temp. even the sample is sintered at different temperatures [fig 3(iii)(iv)] However the sample $Cu_{.4}Zn_{.6}Fe_2O_4$ sintered at $600^\circ C$ shows a slight increase of susceptibility and then continuously decreases with increase of temp.

In the previous discussion on magnetisation, it is stated that at higher content of Zn the magnetisation decreases. This is related to the decrease of A-B interaction and domination of B-B interaction which favours the canting in these materials. Such materials show a continuous decrease of susceptibility with temp. fig.(iii-iv). Similar is the observed result. [25].

The remaining samples shown in figures [3(v-viii)] represent the MD type of behaviour irrespective of their sintering temperatures.

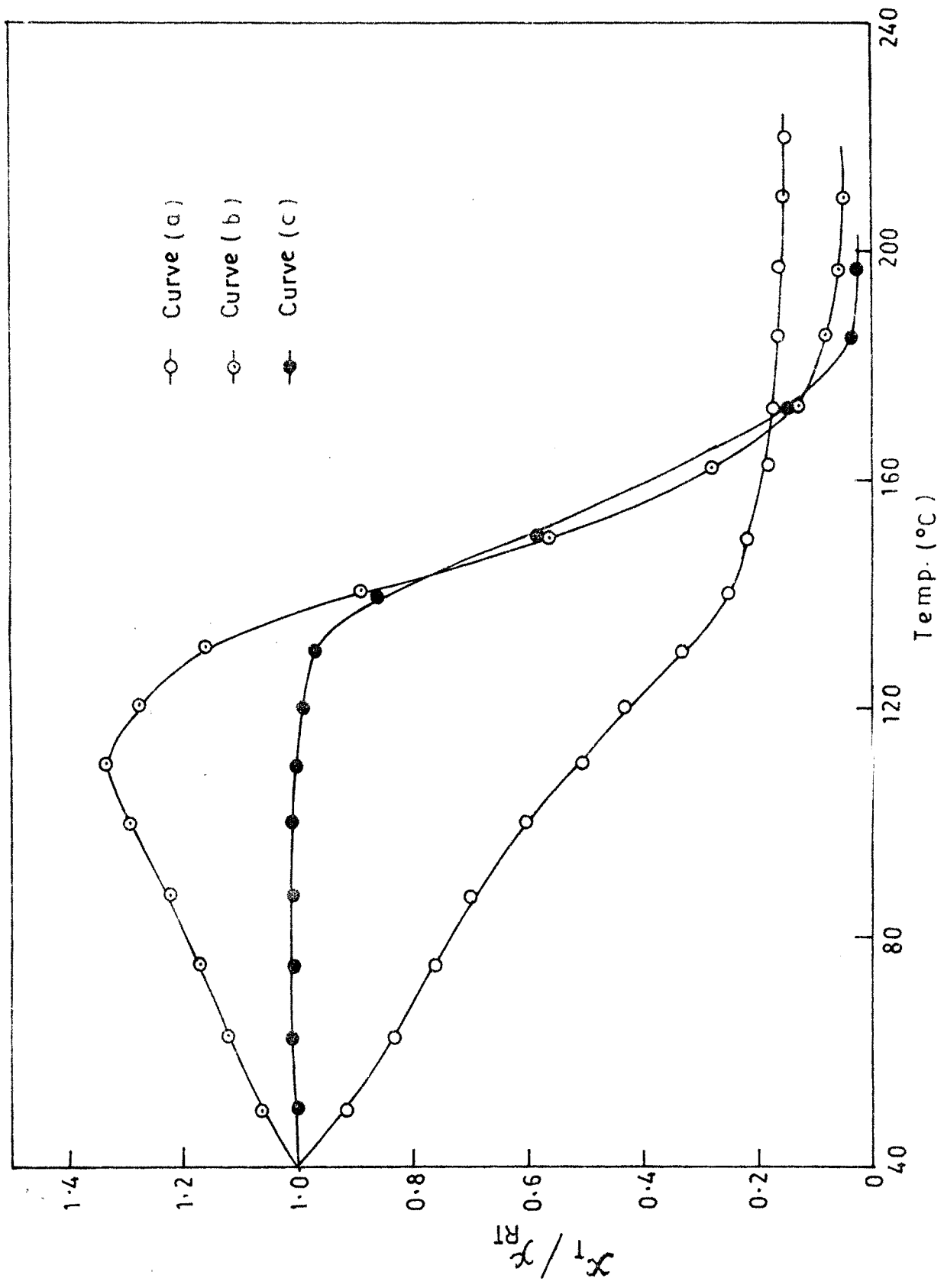


Fig. 3(i) - Variation of χ_T/χ_{RT} Vs T for $Mg_{0.7}Zn_{0.3}Fe_2O_4$ at different sintering temps.

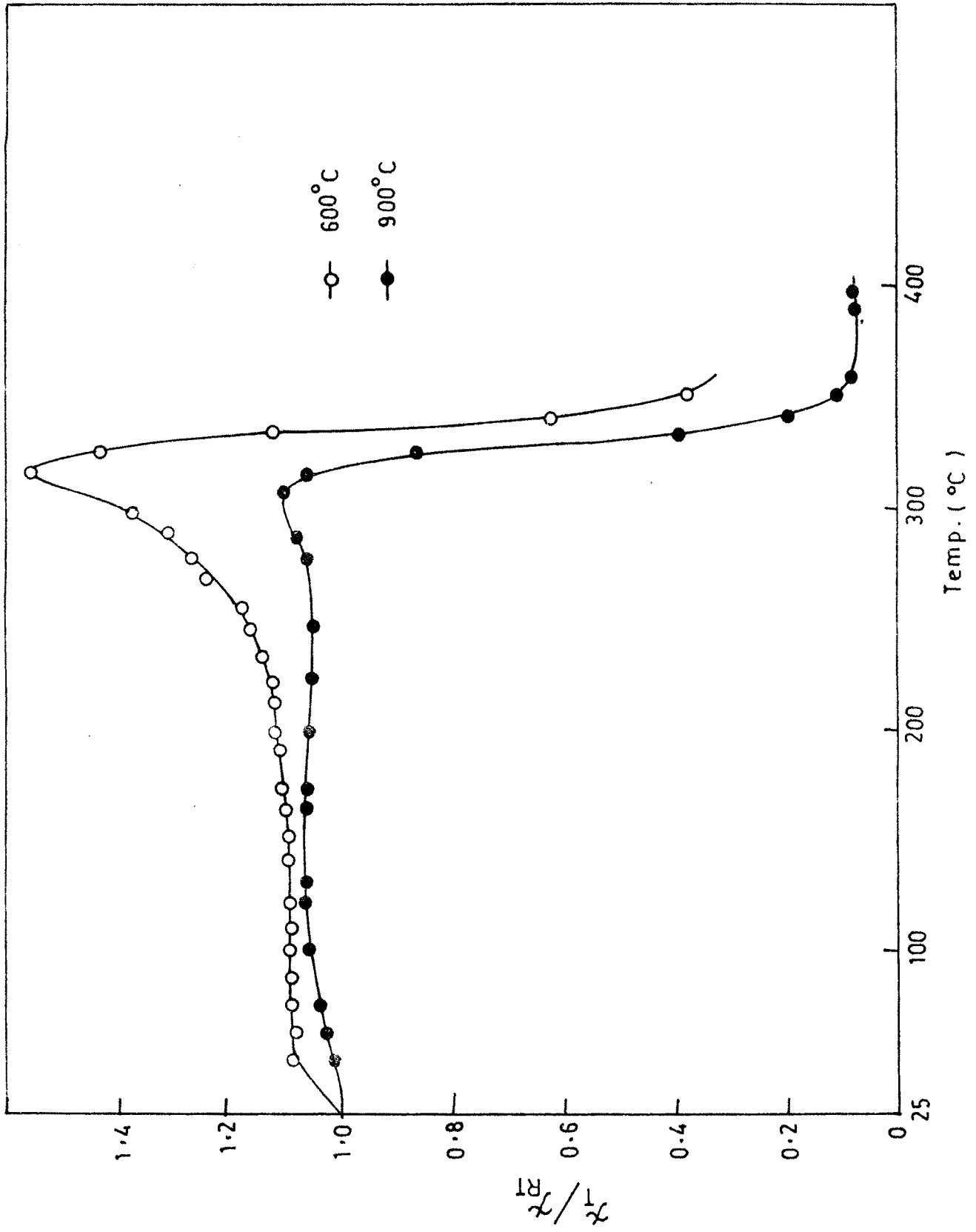


Fig. 3(ii) - Variation of ρ_T/ρ_{RT} Vs T for $Mg_{0.7}Cu_{0.3}Fe_2O_4$ at different sintering temps.

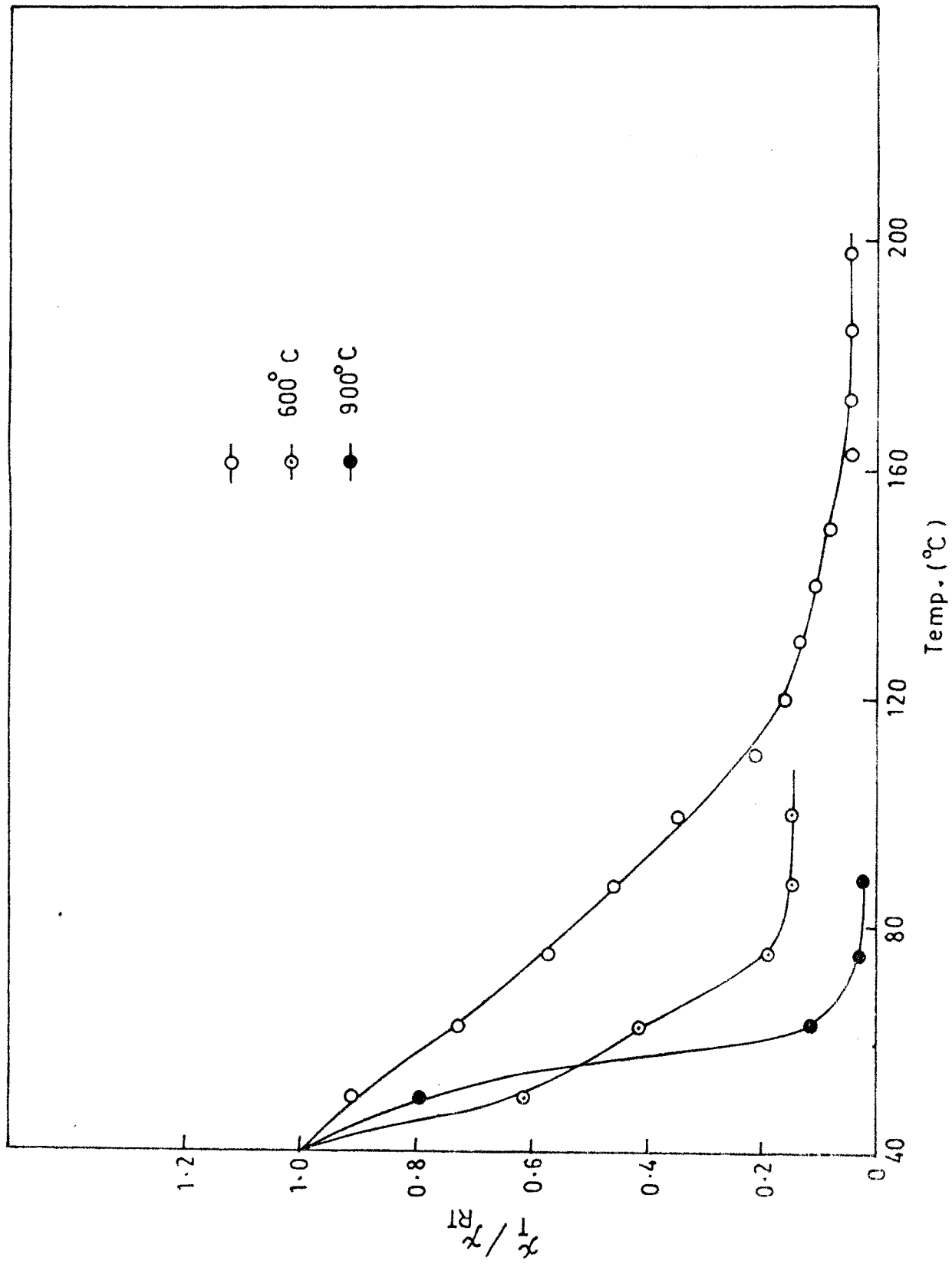


Fig. 3 (iii) - Variation of χ_T/χ_{RT} vs T for $\text{Mg}_{0.4}\text{Zn}_{0.6}\text{Fe}_2\text{O}_4$ at different sintering temps.

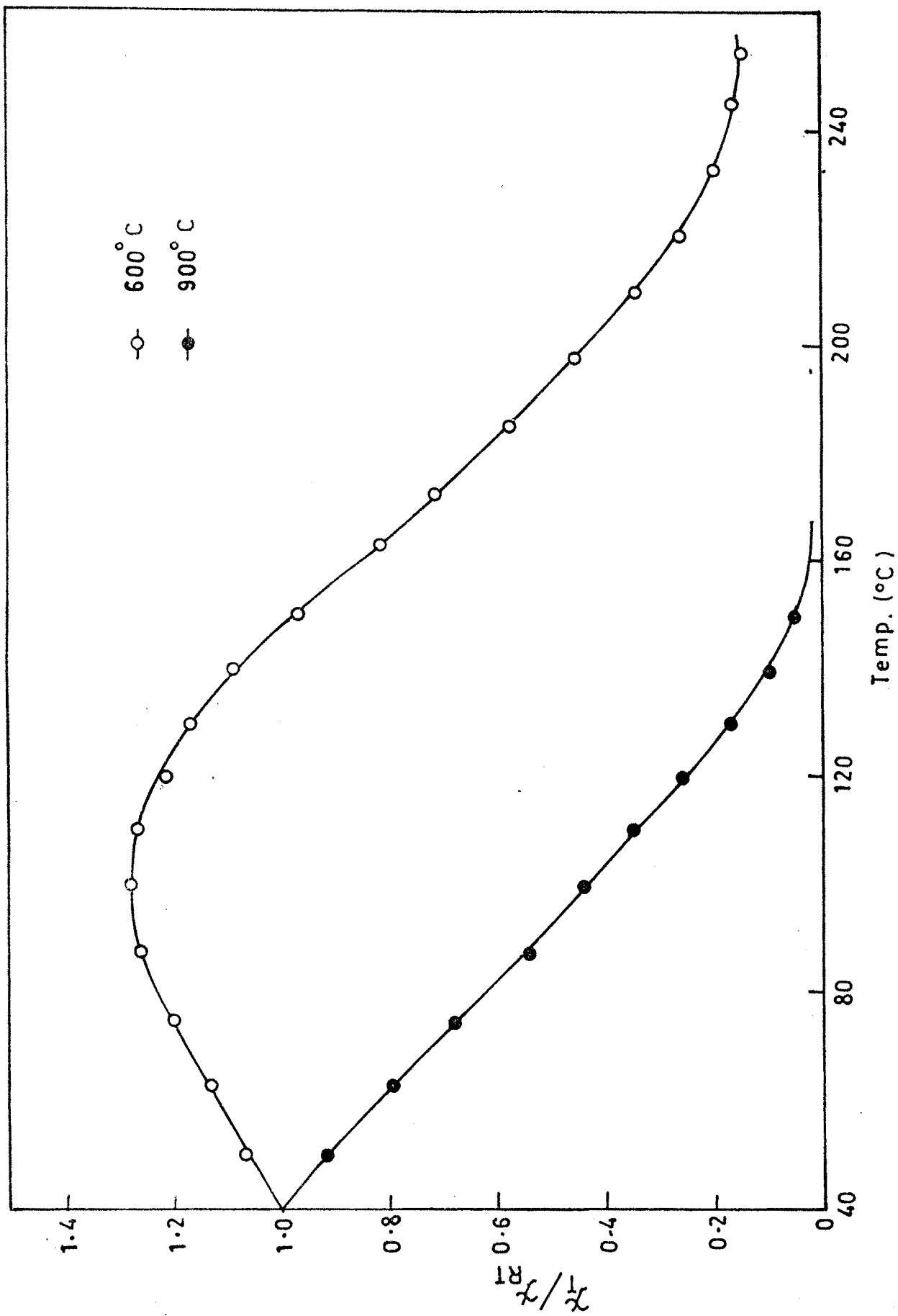


Fig. 3 (iv) - Variation of r/r_{RT} Vs T for $Cu_{0.4}Zn_{0.6}Fe_2O_4$ at different sintering temps -

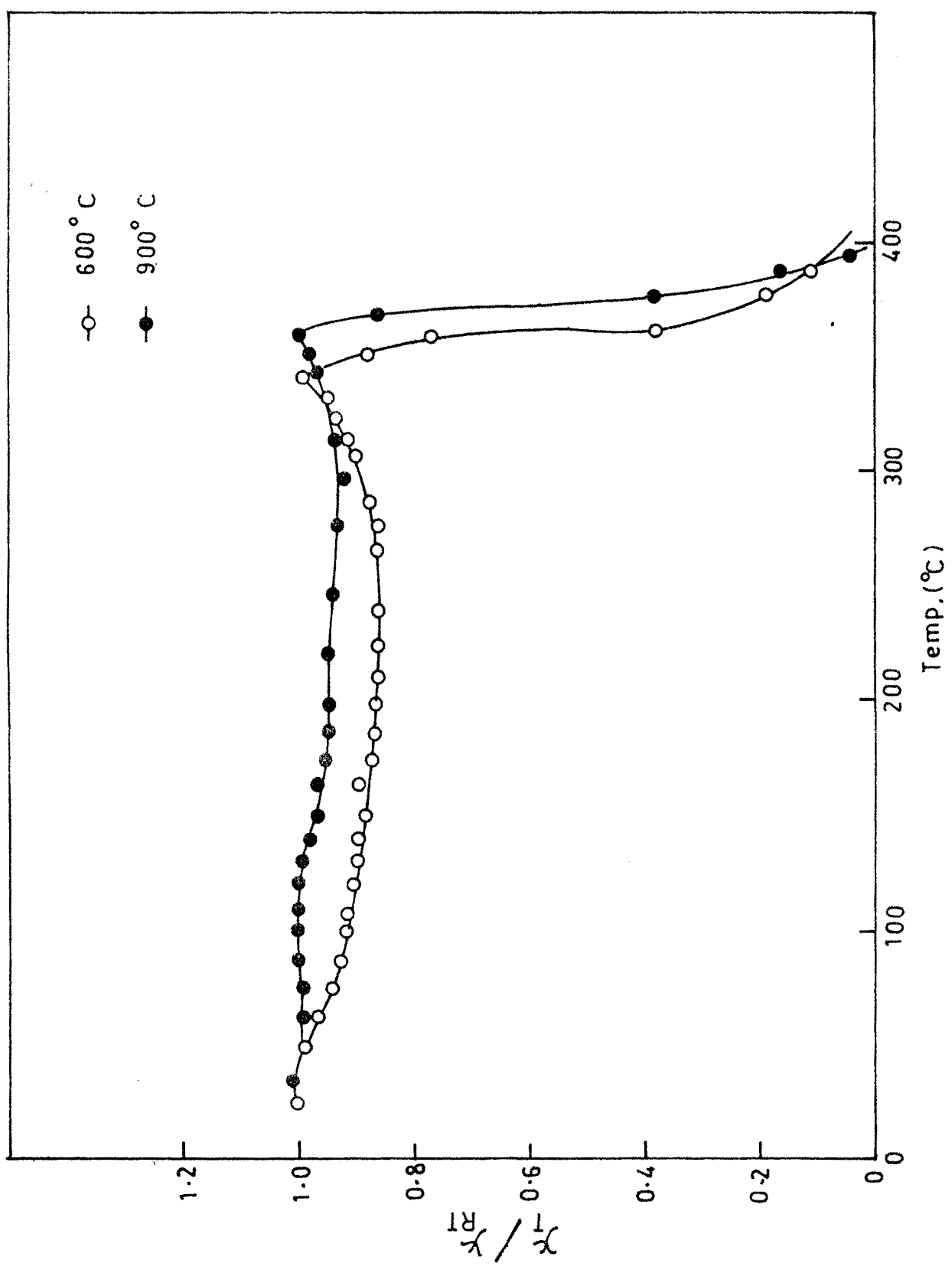


Fig. 3(v) — Variation of χ_{RT} / χ_T Vs T for $Mg_{0.4}Cu_{0.6}Fe_2O_4$ at different sintering temps. 5

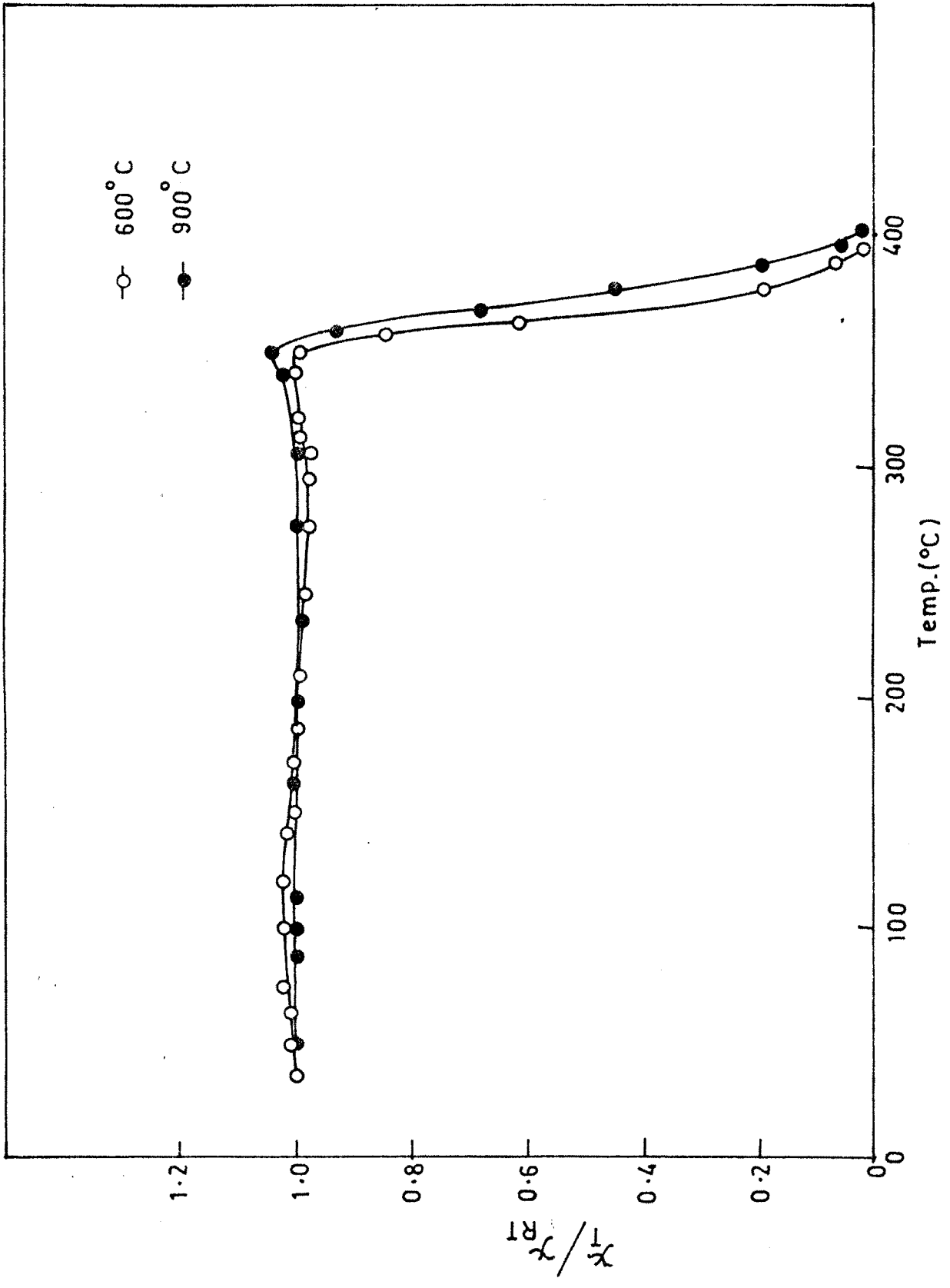


Fig. 3(vi) - Variation of χ_T/χ_{RT} Vs T for CuFe_2O_4 at different sintering temps.

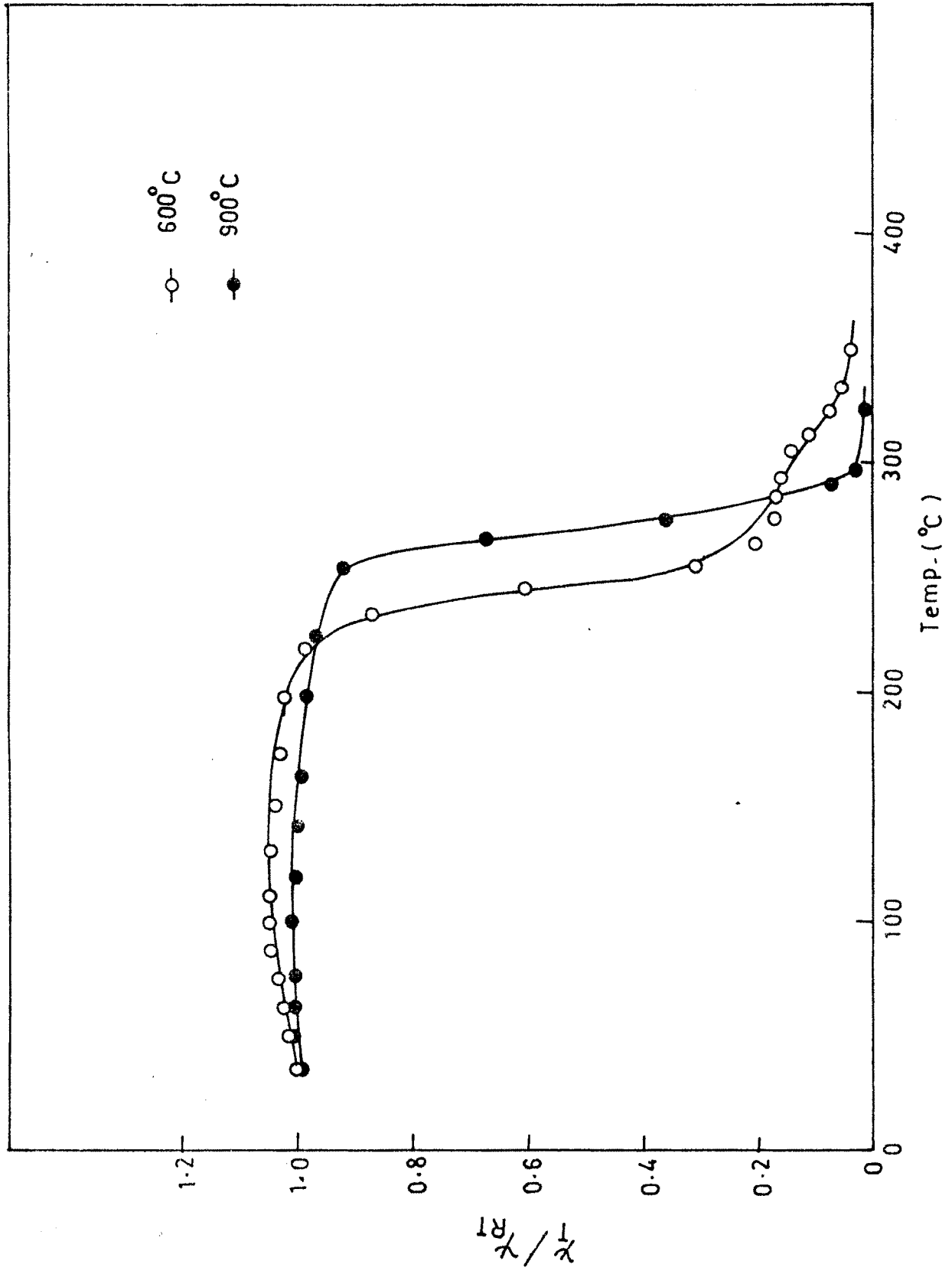


Fig. 3(vii) — Variation of χ/χ_{RT} vs T for $\text{Cu}_{0.7}\text{Zn}_{0.3}\text{Fe}_2\text{O}_4$ at different sintering temps.

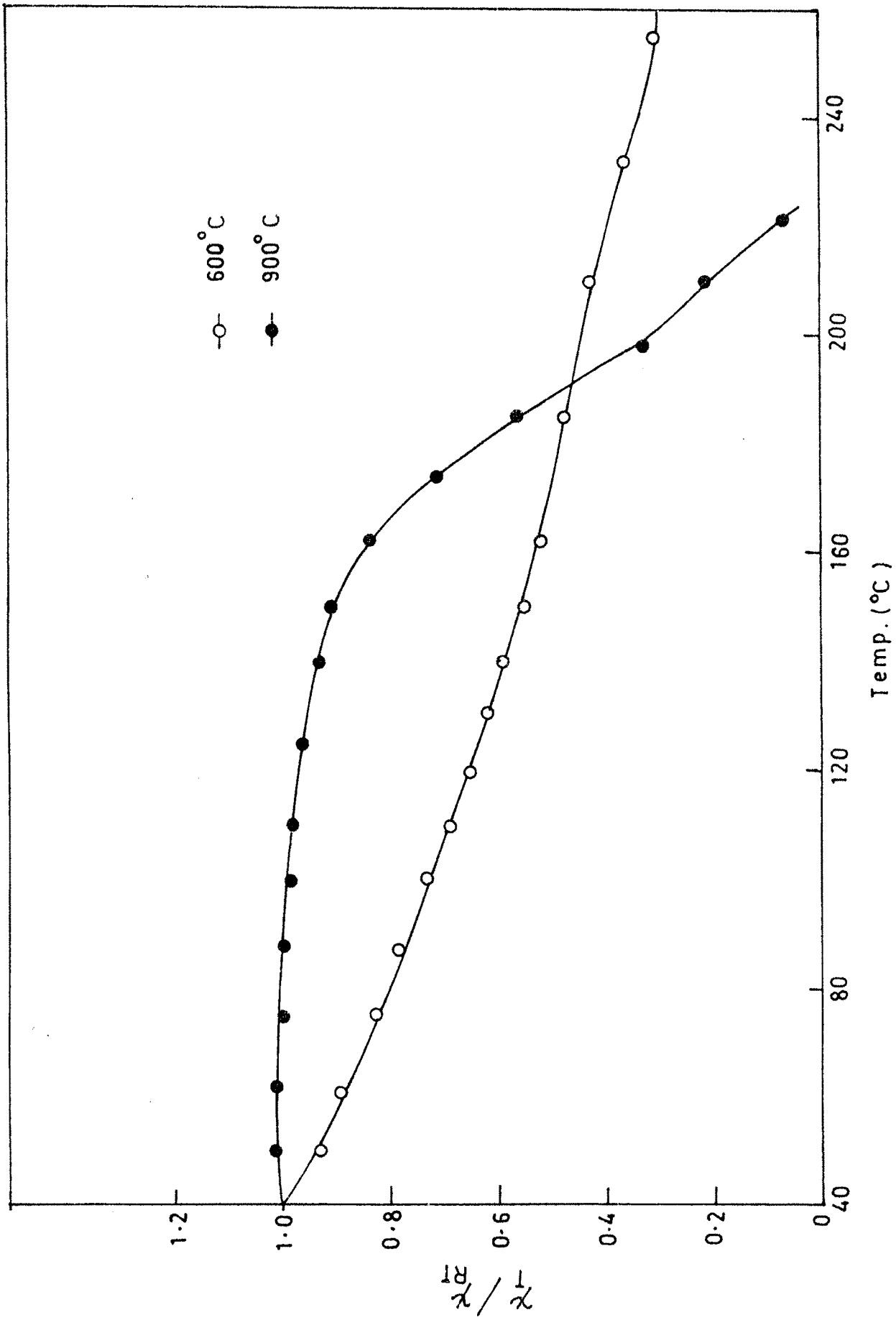


Fig. 3 (viii) - Variation of χ_T / χ_{RT} Vs T for $\text{Mg}_{0.7}\text{Zn}_{0.3}\text{Fe}_2\text{O}_4$ [Mixed] at different sintering temps.

REFERENCES :

1. Weiss P.J. Phy. Theo. Appl. 6 667 (1907)
2. Heisenberg, W., Z. physics. 41, 619(1978)
3. Dormann J.L. and nogus M., J. phys. condn.mat. 2,1223(1990)
4. Gorter, E.W., phillips. res., 9 , 295,(1954)
5. Alex Goldman., "Electronic Ceramics, Prop. Devices and Applications. Ed. Lionel M. Levinson, New York (1998)
6. Alper A.M., 'High tempreture Oxides ' Acad. press. New York(1977)
7. Bean, C.P, J. Appl . phys. 26 ,1381, (1955)
8. Maxwell, s.p., The Marconic, Rev., 1st quarter 20, (1970)
9. Neel, L., Adv, phys. 4 191 (1955)
10. P. J. "Ferromagnetic materials " Ed Wohlforth E.P. (Amsterdam) 2 , 204 (1980).
11. Chakravathy R. Madhav Rao L., Paranjpe S.k., Kulshrestha S.K., Proc . ICF 5, (1989) India.
12. Upadyay R.V., Ind. J. pur and Appl. phys.31 ,333 (1993).
13. Radhakrishnamurthy C, Likhite S. D. , Natrajan R., J. mag. and Mag. mater. 15-18,195 (1980).
14. Miller A.J., Appl . phys. 30 ,248 (1959).
15. Gilileo , M.A.J. phys. chem. solids, 11 , 33 (1960).
16. Radhakrishnamurthy C. , Likhite S.D., and Sahusrabudhe p.w. , proc. Ind. Acad. scl. 87A, 245 (1978)
17. Radhakrishnamurty C., Likhite S.D. and Sastry N.P., Phillips mag. 23, 503, (1971)
18. S. Schikazumi, physics of magnetism, John Wilkey and sons New York 1964
19. Standiey K. J., oxide magnetic materials, Clarendom press, Oxford 1972.

20. Hopkinson J., Philips Trans. Roy. Soc. (London), AL- 80 (1989) 443.
21. Radhakrishnamurthy C., Likhite S.D., Deutsch E. R. and Murthy G. S., Phys. Earth planet Inter; 30 (1982) 281.
22. Stoner E. C. and Wohlfarth E. P., Phil trans. Roy. Soc. 240 A (1948) 599.
23. Vijayaraghavan R. Chougule R. S., Radhakrishnamurthy C., Sampathkumaran E.V., Mullick S. K., Mat. Res. Bull.
24. S.C. Choudhari M.Phil Thesis, "Electrical and magnetic properties of chromium substituted nickel ferrites". Shivaji University, Kolhapur (1993).
25. V. C. Mahajan Ph.D thesis, "Synthesis, Characterisation and substitution", Shivaji University, Kolhapur (1994)